Research Article

# Preparation of $ZrC@Al_2O_3$@Carbon composite aerogel with excellent high temperature thermal insulation performance

Hao Suo[1,2] · Wei Wang[1,2] · Shengjun Jiang[1,2] · Yanhan Li[1,2] · Kewei Yu[1] · Shuntian Huang[1] · Sheng Cui[1,2] · Xiaodong Shen[1,2] · Jun Xue[1]



**Abstract**

The $ZrC@Al_2O_3$@carbon composite aerogels are obtained from low-cost inorganic salt of zirconium and aluminum as raw materials through sol–gel route and carbothermal reduction process. The effects of reactant molar ratios and heat-treatment time on physicochemical properties of $ZrC@Al_2O_3$@carbon composite aerogels are investigated. The results show that the compressive strength of $ZrC@Al_2O_3$@carbon composite aerogel is as high as 1.31 MPa. The specific surface area of sample is as high as 650.4 $m^2\ g^{-1}$, which is beneficial for its application of thermal insulation and catalyst supporting at elevated temperatures. After heat-treated at 1500 °C for 5 h, the thermal conductivity of carbon fiber mat reinforced composite aerogel is as low as 0.048 $W\ m^{-1}\ K^{-1}$ (25 °C).

**Keywords** Composite · Aerogel · Compressive strength · Thermal conductivity · Nanomaterials

## 1 Introduction

Aerogels are high performance material with high specific surface area, ultra-low density and low thermal conductivity [1–3]. Among the various types of aerogels, the oxide aerogels and carbon aerogels have attracted the widest attention. Oxide aerogels mainly include $SiO_2$, $Al_2O_3$, $TiO_2$ and $ZrO_2$ aerogels [4–6], among which the $SiO_2$ aerogels are most extensively studied. $SiO_2$ aerogels have the property of ultra-low density, high porosity and ultra-low thermal conductivity [7]. However, $SiO_2$ aerogels suffer from poor high temperature stability and the decrease of specific surface area when heat treated over 1000 °C [8]. Carbon aerogels possess excellent physicochemical properties with ultra-high specific surface area, low density and high wear resistance [9, 10], enabling it to be widely used in barriers, energy and catalyst supports [11, 12]. Nevertheless, the oxidation of carbon aerogel occurs in ambient atmosphere at as low as 400 °C [13]. Therefore, how to improve the high temperature stability and oxidation resistance of aerogels have attracted interest all over the world.

Zirconium carbide (ZrC) is a typical transition metal carbide with high melting point, extreme hardness and low density [14, 15]. Thus, it has great potential of application in heat resistant insulation materials, electrode materials and coatings field [16, 17]. Li et al. [18] presented a method using polyzirconoxone (PZO) as zirconium source to prepared ZrCO/C composite aerogels. The results showed that the ZrCO/C composite aerogels possessed a higher specific surface area (589 $m^2\ g^{-1}$) than the pure $ZrO_2$ aerogels after heat treatment at 1500 °C. Hence, we predict that the novel $ZrC@Al_2O_3$@carbon aerogels would have the properties of excellent thermal stability and higher compressive strength compared with the traditional $ZrO_2$ aerogels and carbon aerogels.

Herein, we have developed a route combining sol–gel method with $CO_2$ supercritical fluid drying technique to

✉ Sheng Cui, scui@njtech.edu.cn | [1]Department of Materials Science and Engineering, Nanjing Tech University, Nanjing 210009, People's Republic of China. [2]Jiangsu Collaborative Innovation Center for Advanced Inorganic Function Composites, Nanjing Tech University, Nanjing 210009, People's Republic of China.

SN Applied Sciences (2019) 1:461 | https://doi.org/10.1007/s42452-019-0478-4

Received: 11 March 2019 / Accepted: 10 April 2019 / Published online: 16 April 2019

synthesis ZrC@$Al_2O_3$@carbon composite aerogels. The composite aerogel was prepared by mixing independently prepared $ZrO_2/Al_2O_3$ sol and RF sol in one pot, followed by solvent exchange, $CO_2$ supercritical drying and carbothermal reduction under flowing argon. The effects of different Zr/Al/R molar ratios and heat-treatment time on the physical and chemistry properties of ZrC@$Al_2O_3$@carbon aerogels are investigated in detail.

## 2 Experimental

### 2.1 Synthesis

$ZrOCl_2{\cdot}8H_2O$, $AlCl_3{\cdot}6H_2O$, EtOH and water were directly mixed with a molar ratio of 1:1:15:55, stirring to prepare $ZrO_2/Al_2O_3$ sol. Resorcinol (R), formaldehyde (F) and water were directly mixed with a molar ratio of 1:2:60, stirring to prepare RF sol. Then, $ZrO_2/Al_2O_3$ sol, RF sol and PO were mixed with a molar ratio of 1:(2, 3, 4):4, and the mixture was put into new beaker. The wet gels were aged at 50 °C for 1 day and the aged gels were soaked with ethanol for 5 day. The wet gels were dried with supercritical fluid $CO_2$ to form $ZrO_2/Al_2O_3$/RF composite aerogels. Finally, the $ZrO_2/Al_2O_3$/RF composite aerogels were transformed into the ZrC@$Al_2O_3$@carbon composite aerogels by calcined at 1500 °C under flowing argon. The sample was heat treated in air at 650 °C for 3 h.

### 2.2 Characterizations

X-ray diffraction (XRD) patterns were performed by Cu$K\alpha_1$ radiation (λ = 0.15406 nm) with a Rigaku Miniflex-600. Thermal gravimetric analysis (TGA) and differential scanning calorimetry analysis (DSC) patterns were recorded using a NETZSCH STA449C. Scanning electron microscopy (SEM) was carried out on a LEO-1530VP field emission scanning electron microscope. Transmission electron microscopy (TEM) was carried out on a JEOL JEM-2100 (HR) operating (200 kV). Infrared spectrum was investigated with a Nicolet Avatar IS-5. The thermal conductivity analysis was carried out on a Hot Disk-2500 thermal constant analyzer. $N_2$ adsorption/desorption and pore distribution were obtained by using a Micromeritics ASAP2020.

## 3 Results and discussion

As is shown in Fig. 1, the $ZrO_2/Al_2O_3$/RF composite aerogels are transformed into black-colored ZrC@$Al_2O_3$@carbon composite aerogels after calcined at 1500 °C. Due to the pyrolysis of organic constitutes, the linear shrinkage of ZrC@$Al_2O_3$@carbon composite aerogels are evidently observed during the carbonization process [19]. Table 1 shows that the bulk densities of composite aerogel undergo a decrease-increase trend with the increase of Zr/R molar ratios. The gelation time of ZrC@$Al_2O_3$@carbon composite aerogels are determined by the gelation rate of both $ZrO_2$ and $Al_2O_3$ gel, and the gelation time of $ZrO_2/Al_2O_3$ gels are shorter than RF gel. PO is an effective proton capture agent which can slowly consume the $H^+$ protons in $H_2O$ and its ring-opening reaction can promote the hydrolysis and polycondensation reaction of $[Zr_4(OH)_8{\cdot}(H_2O)_{16}]^{4+}$ and $[Al(H_2O)_6]^{3+}$ [20, 21]. It is noted that the mechanical strength of ZrC@$Al_2O_3$@carbon composite aerogel is higher than the oxide aerogel after carbothermal reduction process. The compressive strength is as high as 1.31 MPa, which is higher than ZrCO composite aerogel (0.87 MPa) [14].

Figure 2a exhibits the XRD patterns of the composite aerogels (Zr:Al:R = 1:1:3) calcinated at 1500 °C with different heat-treated time. With the increase of treatment time, the characteristic peak intensity of tetragonal $ZrO_2$ phase (t-$ZrO_2$) decrease, indicating the phase transition of $ZrO_2$. It is also well known that the γ-$Al_2O_3$ phase can be transformed into α-$Al_2O_3$ above 1000 °C [22, 23]. It is worth noting that the characteristic peaks of tetragonal $ZrO_2$ phase and γ-$Al_2O_3$ phase still exist in the composites after heat-treated at 1500 °C for 5 h, which can be ascribed to the inability of $ZrO_2/Al_2O_3$ nucleus growth caused by the coating of the carbon aerogel particles on the surface of the $ZrO_2/Al_2O_3$ crystals. With a higher heat-treated time at 1500 °C for 10 h, the t-$ZrO_2$ phase almost disappear, and the intensity of ZrC phase is maximized. Figure 2a exhibits the XRD patterns of the composite aerogels (Zr:Al:R = 1:1:3) calcinated at 1500 °C for 3 h. As is shown in Fig. 2b, the weight loss of preliminary stage is about 15% with an endothermic peak at 65 °C, which is mainly due to the evaporation of ethanol and physically adsorbed water [24]. The obvious exothermic peak in the second stage at 550 °C with a weight loss of 23% is mainly caused by continuous structural transition from boehmite to γ-$Al_2O_3$. The third region where a weak exothermic peak in the DSC curve at ca. 1020 °C, arise from the carbonization reaction of the composite aerogel with a corresponding weight loss of 5%. A significant weight losses occur in the last region, which corresponds to the structure transition of $ZrO_2$ and a part of the formation of ZrC as is shown in Eq. (1) [25]. The results are consistent with the results of XRD analysis.

$$ZrO_2 + 3C \rightarrow ZrC(s) + 2CO(g) \quad (1)$$

In order to understand the microstructure of the composite aerogel, Fig. 3 shows the SEM and TEM images of the composite aerogels (Zr:Al:R = 1:1:3) calcinated at 1500 °C with different heat treatment time. As is shown in Fig. 3a, d, g, we can see that the ZrC@$Al_2O_3$@carbon

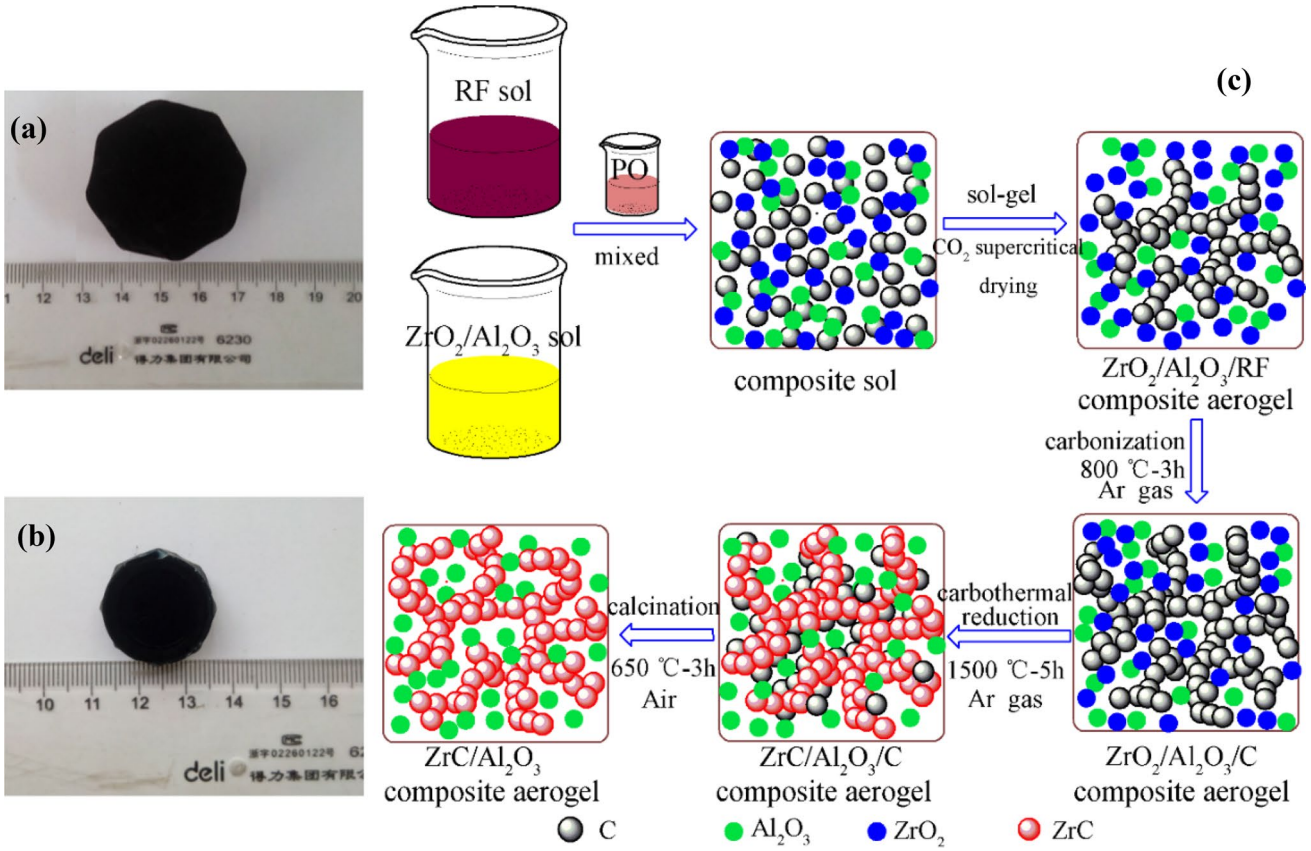


**Fig. 1** Photographs of **a** $ZrO_2/Al_2O_3$/RF, **b** $ZrC@Al_2O_3$@carbon composite aerogel and **c** schematic representation of growth mechanism of composite aerogel

**Table 1** The physical properties of $ZrC@Al_2O_3$@carbon composite aerogels calcining at 1500 °C for 3 h with different Zr/Al/R molar ratios

| Zr/Al/R molar ratio | Gelation time (t $min^{-1}$) | Bulk density (g $cm^{-3}$) | Compressive strength (MPa) |
|---|---|---|---|
| 1:1:2 | 5 | 0.322 | 1.15 |
| 1:1:3 | 12 | 0.239 | 1.22 |
| 1:1:4 | 18 | 0.267 | 1.18 |
| 1:2:4 | 10 | 0.301 | 1.31 |

composite aerogels possess a network structure of connected nanoparticles after heat treatment at 1500 °C. The structure of $ZrC@Al_2O_3$@carbon composite aerogel is disordered but homogenious, with the scale of approximately 40 nm. It is mainly formed by different hydrolysis and condensation rate of $ZrO_2/Al_2O_3$ and RF sol. Figure 3a, d, g show that the colloidal particle diameters are around 80 nm and the smallest nanopores have the diameters of around 40–70 nm after carbothermal at 1500 °C for 5 h. With the increase of heat-treatment time, nanoparticles adjoin more closely to each other and a certain amount of large pores with diameters greater than 200 nm emerge in composite aerogels, mainly caused by the consumption of the $ZrO_2$ by its further reaction with RF aerogel. As is shown in Fig. 3b, e, h, a layer of graphitized carbon exist on the surface of composite aerogel and γ-$Al_2O_3$ inside the aerogel after heat treatment at 1500 °C. With the increase of heat-treatment time, the quantity and size of polygonal particles increase and the structural transition of composite occurs. As shown in Fig. 3h, i, the γ-$Al_2O_3$ phase has ca.45 nm length and the grain growth inside the composite aerogel can be observed after heat treatment at 1500 °C for 10 h.

Figure 4 shows the nitrogen sorption isotherms of $ZrC@Al_2O_3$@carbon composite aerogels heat-treated at 1500 °C for 3 h with different Zr/Al/R molar ratios. The curves include type IV curves with type H1 hysteresis loop in the IUPAC classification, which is correspondent to the mesoporous structure with cylindrical pores.

Table 2 presents that with the increase of R/Zr molar ratio, the specific surface areas and average pore diameter undergo an increase–decrease trend. When the R/Zr molar ratio is 3, the BET specific surface areas of composite aerogel is as high as 650.4 $m^2 g^{-1}$. This phenomenon is mainly caused by the structural adjustment, damage to the

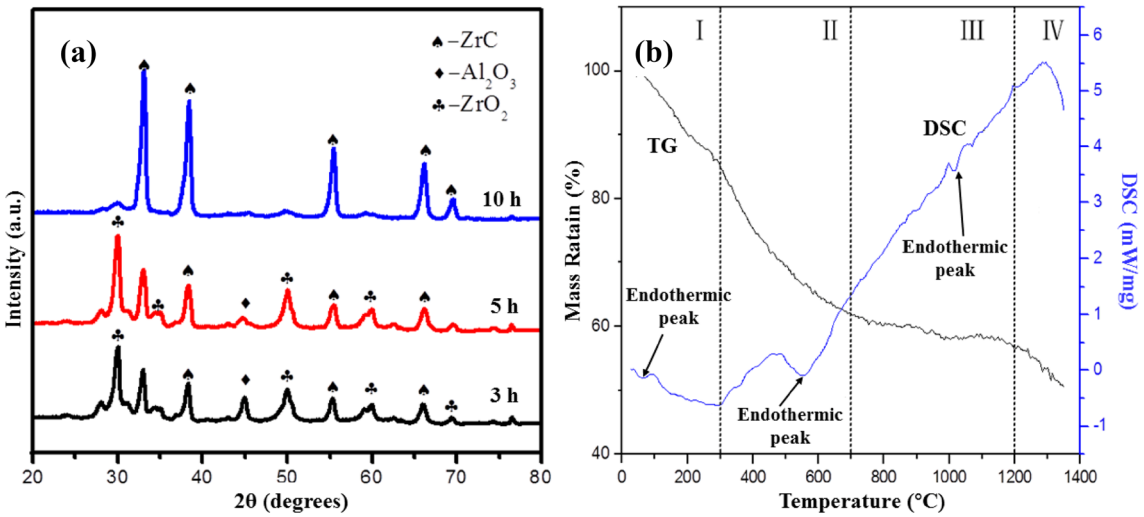


**Fig. 2** XRD patterns **a** and TG and DSC curves **b** of ZrC@$Al_2O_3$@carbon composite aerogel (Zr:Al:R = 1:1:3) calcining at 1500 °C

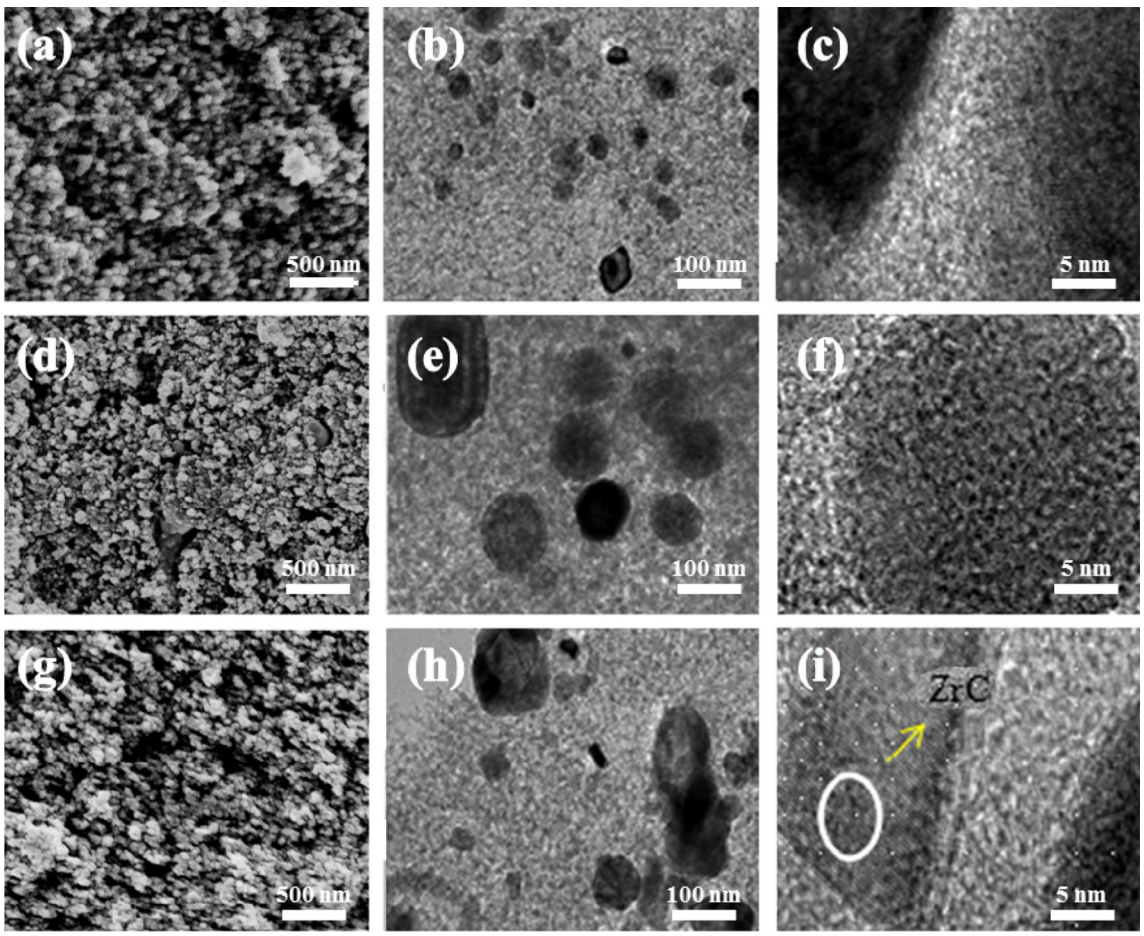


**Fig. 3** SEM **a**, **d**, **g** and TEM **b**–**c**, **e**–**f**, **h**–**i** images of ZrC@$Al_2O_3$@carbon composite aerogel with different heat treatment time: **a**–**c** 1500 °C-3 h; **d**–**f** 1500 °C-5 h; **g**–**i** 1500 °C-10 h

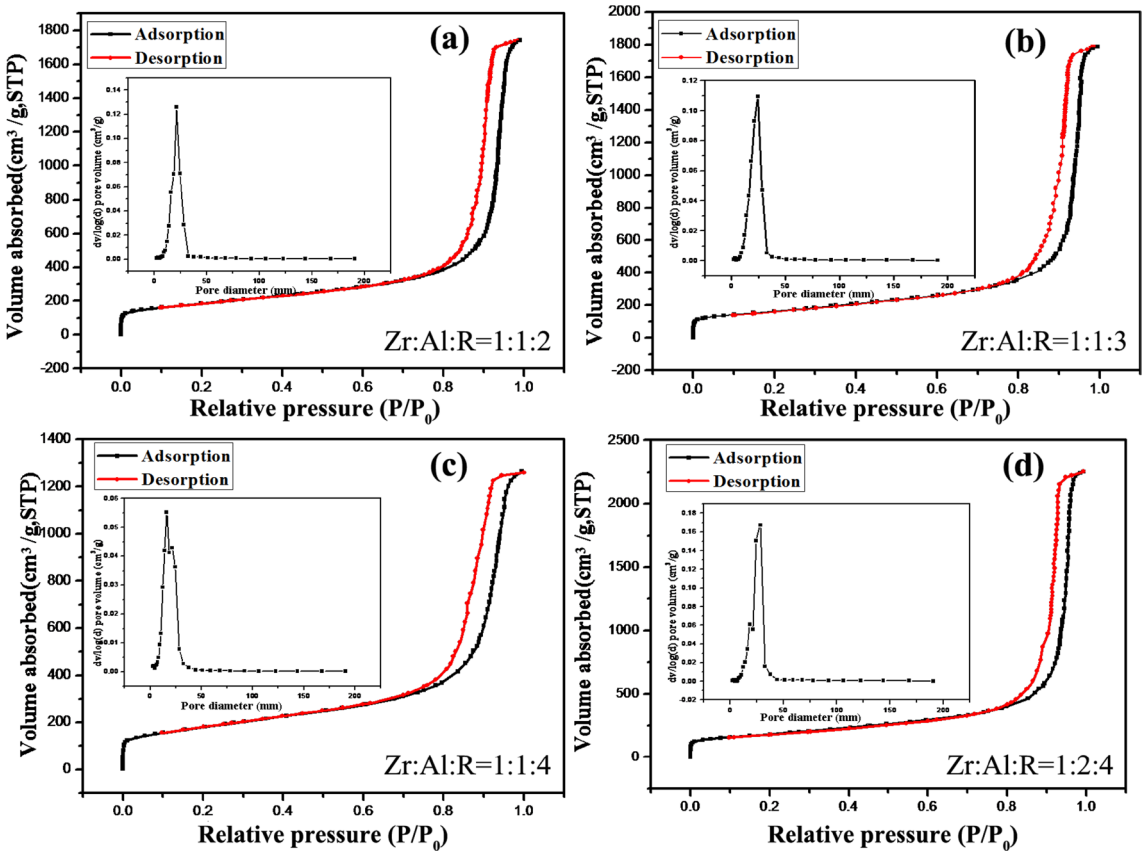


**Fig. 4** Nitrogen sorption isotherms of ZrC@$Al_2O_3$@carbon composite aerogel heat-treated at 1500 °C for 3 h with different Zr/Al/R molar ratios

**Table 2** Pore structures of ZrC@$Al_2O_3$@carbon composite aerogels heat treated at 1500 °C for 3 h with different Zr/Al/R molar ratios

| Zr/Al/R molar ratio | Specific surface area ($m^2\ g^{-1}$) | Average pore diameter (nm) |
|---|---|---|
| 1:1:2 | 570.1 | 16.5 |
| 1:1:3 | 650.4 | 19.3 |
| 1:1:4 | 636.1 | 12.3 |
| 1:2:4 | 631.7 | 21.8 |

**Table 3** Bulk density and thermal conductivity of carbon fiber mat reinforced ZrC@$Al_2O_3$@carbon composite aerogel with different heat-treatment time

| Sample | Carbon fiber mat | A | B | C | D |
|---|---|---|---|---|---|
| Bulk density ($g\ cm^{-3}$) | 0.135 | 0.195 | 0.184 | 0.178 | 0.176 |
| Thermal conductivity (25 °C, $W\ m^{-1}\ K^{-1}$) | 0.063 | 0.051 | 0.048 | 0.061 | 0.057 |

A, B, C present the carbon fiber mat reinforced ZrC@$Al_2O_3$@carbon composite aerogel after heat-treated at 1500 °C for 3 h, 5 h and 10 h; D presents the carbon fiber mat reinforced ZrCO composite aerogel heat-treatment at 1500 °C for 3 h

porous network and shrinkage of the pore structure. The specific surface area of composite aerogel is larger than the ZrCO composite aerogel (637.4 $m^2\ g^{-1}$), which is beneficial for applications in thermal insulations areas upon heat treatment over 1200 °C. With the increase of Al/Zr molar ratio, the average pore diameters are below 25 nm and the average pore diameter is as small as 21.8 nm with the Zr/Al/R molar ratio of 1:2:4.

Table 3 shows the bulk density and thermal conductivity of carbon fiber mat reinforced ZrC@$Al_2O_3$@carbon composite aerogel with different heat-treatment time. In order to improve the poor mechanical properties of aerogels, they are reinforced with carbon fiber. Also, the addition of γ-$Al_2O_3$ phase is beneficial for improving the comprehensive performance of the composite aerogel, such as high thermal stability and low volume shrinkage. The thermal conductivity of carbon fiber reinforced composite aerogel undergo a decrease-increase trend. After heat treatment at 1500 °C for 5 h, the thermal conductivity of sample is 0.051 $W\ m^{-1}\ K^{-1}$. With the increase of heat treatment time, nanoparticles adjoin more closely to each other, and the

composite aerogel exhibits a compact mesoporous network, in which the pore size become smaller. Meanwhile, graphitized carbon on the surface of composite aerogel can effectively reduce the rates of heat transfer, which is beneficial to reduce the thermal conductivity of aerogel. However, with a further heat treatment time for 10 h, a small amount of large pores (200 nm) emerge in the composite aerogel, which is not favorable to low thermal conductivity of the composite aerogel. After heat-treated at 1500 °C for 5 h, the thermal conductivity of carbon fiber reinforced composite aerogel is as low as 0.048 W $m^{-1}$ $K^{-1}$ (25 °C), which is obviously lower than that of the pure carbon fiber mat (0.063 W $m^{-1}$ $K^{-1}$, 25 °C) and ZrCO composite aerogel (0.057 W $m^{-1}$ $K^{-1}$) [14].

## 4 Conclusions

In summary, we have developed a sol–gel method combined with $CO_2$ supercritical fluid drying technique to synthesis ZrC@$Al_2O_3$@carbon composite aerogel using economical inorganic salt of zirconium and aluminum. The addition of γ-$Al_2O_3$ phase is beneficial for improving the comprehensive properties of composite aerogel including high thermal stability and low volume shrinkage. The BET specific surface area of composite aerogel is as high as 650.4 $m^2$ $g^{-1}$, and the thermal conductivity of carbon fiber mat reinforced composite aerogel is as low as 0.048 W $m^{-1}$ $K^{-1}$ (25 °C), which is beneficial to the applications of thermal insulations and catalyst supporting at elevated temperatures.

**Acknowledgements** This work was financially supported by the Industry Program of Science and Technology Support Project of Jiangsu Province (BE2016171, BE2017151), the Major Program of Natural Science Fund in Colleges and Universities of Jiangsu Province (15KJA430005), the Program for Changjiang Scholars and Innovative Research Team in University (No. IRT_15R35), and the Priority Academic Program Development of Jiangsu Higher Education Institutions (PAPD).

### Compliance with ethical standards

**Conflict of interest** The authors declare that they have no conflict of interest.

## References

1. Lermontov SA, Sipyagina NA, Malkova AN et al (2016) Chiral lactate-modified silica aerogels. Microporous Mesoporous Mater 237:127–131
2. Suo H, Peng CX, Jing F et al (2019) Facile preparation of $TiO_2$/ZnO composite aerogel with excellent antibacterial activities. Mater Lett 2019(234):253–256
3. Wu XD, Shao GF, Shen XD et al (2017) Evolution of the novel C/$SiO_2$/SiC ternary aerogel with high specific surface area and improved oxidation resistance. Chem Eng J 330:1022–1034
4. Laskowski J, Milow B, Ratke L (2016) Aerogel–aerogel composites for normal temperature range thermal insulations. J Non Cryst Solids 441:42–48
5. Shi Z, Gao H, Wang X et al (2017) One-step synthesis of monolithic micro-nano yttria stabilized $ZrO_2$–$Al_2O_3$ composite aerogel. Microporous Mesoporous Mater 259:26–32
6. Nawaz M, Miran W, Jang J et al (2017) One-step hydrothermal synthesis of porous 3D reduced graphene oxide/$TiO_2$ aerogel for carbamazepine photodegradation in aqueous solution. Appl Catal B Environ 203:85–95
7. He J, Li X, Su D et al (2016) Ultra-low thermal conductivity and high strength of aerogels/fibrous ceramic composites. J Eur Ceram Soc 36:1487–1493
8. Zhong Y, Zhang J, Wu XD et al (2017) Carbon-fiber felt reinforced carbon/alumina aerogel composite fabricated with high strength and low thermal conductivity. J Sol Gel Sci Technol 2017(84):129–134
9. Pekala RW (1989) Organic aerogels from the polycondensation of resorcinol with formaldehyde. J Mater Sci 24:3221–3227
10. Sun H, Xu Z, Gao C (2013) Multifunctional, ultra-flyweight, synergistically assembled carbon aerogels. Adv Mater 25:2554–2560
11. Feng J, Zhang C, Feng J (2012) Carbon fiber reinforced carbon aerogel composites for thermal insulation prepared by soft reinforcement. Mater Lett 67:266–268
12. Liu W, Li X, Zhu M et al (2015) High-performance all-solid state asymmetric supercapacitor based on $Co_3O_4$ nanowires and carbon aerogel. J Power Sour 282:179–186
13. Seraji MM, Ghafoorian NS, Bahramian AR et al (2015) Preparation and characterization of C/$SiO_2$/SiC aerogels based on novolac/silica hybrid hyperporous materials. J Non Cryst Solids 425:146–152
14. Cui S, Suo H, Jing F et al (2018) Facile preparation of ZrCO composite aerogel with high specific surface area and low thermal conductivity. J Sol Gel Sci Technol 86:383–390
15. Cetinkaya S (2017) Synthesis of fine zirconium carbide powder by carbothermal reaction of carbon-coated zirconia particles. J Am Ceram Soc 100:5444–5449
16. Shi XH, Huo JH, Zhu JL et al (2014) Ablation resistance of SiC–ZrC coating prepared by a simple two-step method on carbon fiber reinforced composites. Corros Sci 88:49–55
17. Sun W, Xiong X, Huang BY et al (2009) ZrC ablation protective coating for carbon/carbon composites. Carbon 47:3368–3371
18. Ye L, Qiu W, Li H et al (2013) Preparation and characterization of ZrCO/C composite aerogels. J Sol Gel Sci Technol 65:150–159
19. Guo Q, Li J, Shen Q et al (2015) Effect of ball milled Zr/Al/$ZrB_2$ composite powders on microstructure and toughening of $ZrB_2$–SiC/Zr–Al–C composite ceramics sintered by spark plasma sintering. Mater Sci Eng A 644:96–104
20. Wu XD, Zhong Y, Kong Y et al (2015) Preparation and characterization of C/$Al_2O_3$ composite aerogel with high compressive strength and low thermal conductivity. J Porous Mater 22:1235–1243
21. Du A, Zhou B, Zhang Z et al (2013) A special material or a new state of matter: a review and reconsideration of the aerogel. Materials 6:941–968
22. Wu XD, Shao GF, Shen XD et al (2016) Novel $Al_2O_3$–$SiO_2$ composite aerogels with high specific surface area at elevated temperatures with different alumina/silica molar ratios prepared by a non-alkoxide sol–gel method. RSC Adv 6:5611–5620
23. Zhang R, Ye C, Wang B (2017) Novel $Al_2O_3$–$SiO_2$ aerogel/porous zirconia composite with ultra-low thermal conductivity. J Porous Mater 25:171–178

24. Wu XD, Shao GF, Shen XD et al (2016) Synthesis of a novel $Al_2O_3$–$SiO_2$ composite aerogel with high specific surface area at elevated temperatures using inexpensive inorganic salt of aluminum. Ceram Int 42:874–882
25. Sondhi A, Morandi C, Reidy RF et al (2013) Theoretical and experimental investigations on the mechanism of carbothermal reduction of zirconia. Ceram Int 39:4489–4497